


In situ Fabrication of Nano ZnO/BCM Biocomposite Based on MA Modified Bacterial Cellulose Membrane for Antibacterial and Wound Healing

This article was published in the following Dove Press journal:
International Journal of Nanomedicine

Zhenghui Luo^{1,*}

Jie Liu^{1,*}

Hai Lin¹ 


Xi Ren¹

Hao Tian¹

Yi Liang¹

Weiyi Wang¹

Yuan Wang¹

Meifang Yin¹ 

Yuesheng Huang¹

Jiaping Zhang¹

¹Department of Plastic Surgery, State Key Laboratory of Trauma, Burns and Combined Injury, Southwest Hospital, The Third Military Medical University (Army Medical University), Chongqing 400038, People's Republic of China;

²Engineering Research Center in Biomaterials, Sichuan University, Chengdu 610065, People's Republic of China

*These authors contributed equally to this work

Background: Developing an ideal wound dressing that meets the multiple demands of safe and practical, good biocompatibility, superior mechanical property and excellent antibacterial activity is highly desirable for wound healing. Bacterial cellulose (BC) is one of such promising class of biopolymers since it can control wound exudates and can provide moist environment to a wound resulting in better wound healing. However, the lack of antibacterial activity has limited its application.

Methods and Results: We prepared a flexible dressing based on a bacterial cellulose membrane and then modified it by chemical crosslinking to prepare in situ synthesis of nZnO/BCM via a facile and eco-friendly approach. Scanning electron microscopy (SEM) results indicated that nZnO/BCM membranes were characterized by an ideal porous structure (pore size: 30~ 90 μm), forming a unique string-beaded morphology. The average water vapor transmission of nZnO/BCM was 2856.60 $\text{g}/\text{m}^2/\text{day}$, which improved the moist environment of nZnO/BCM. ATR-FITR further confirmed the stepwise deposition of nano-zinc oxide. Tensile testing indicated that our nanocomposites were flexible, comfortable and resilient. Bacterial suspension assay and plate counting methods demonstrated that 5wt. % nZnO/BCM possessed excellent antibacterial activity against *S. aureus* and *E. coli*, while MTT assay demonstrated that they had no measurable cytotoxicity toward mammalian cells. Moreover, skin irritation test and histocompatibility examination supported that 5wt. % nZnO/BCM had no stimulation to skin and had acceptable biocompatibility with little infiltration of the inflammatory cells. Finally, by using a bacteria-infected (*S. aureus* and *E. coli*) murine wound model, we found that nZnO/BCM could prevent in vivo bacterial infections and promote wound healing via accelerating the re-epithelialization and wound contraction, and these membranes had no obvious toxicity toward normal tissues.

Conclusion: Therefore, the constructed nZnO/BCM has great potential for biomedical applications as an efficient antibacterial wound dressing.

Keywords: bacterial cellulose, nano-zinc oxide, in situ synthesis, antibacterial, non-toxicity, wound dressing

Correspondence: Jiaping Zhang
Department of Plastic Surgery, State Key Laboratory of Trauma, Burns and Combined Injury, Southwest Hospital, The Third Military Medical University (Army Medical University), Chongqing 400038, People's Republic of China
Tel +86 23-68754353
Email japzhang@aliyun.com

Introduction

Wound dressings are used to promote a suitable environment for wound healing and protect the damaged tissue from the environment and bacterial infiltration.^{1,2} Due to an increasing number of people suffering from burns, trauma, or diabetic ulcers, etc., the demand for better dressings is growing dramatically.^{3,4} Nowadays, various types of modern dressing materials, including semi-permeable films, hydrogels,

electrospun scaffolds, alginates and so on, have been developed.⁵⁻⁷ However, available commercial wound dressings in use are mostly expensive, poor mechanical performance, or unsuitable water vapor transmission, where wound healing was delayed.^{8,9} Some of these materials even would be leading to maceration and bacterial proliferation, whereas most of these lack antibacterial activity.¹⁰ An ideal wound dressing should be safe and practical, biocompatibility, high tensile strength and modulus, efficient bactericidal activity and suitable permeability for gas and water exchange.¹¹⁻¹⁴

Bacterial cellulose (BC) is one of such promising class of biopolymers since it can control wound exudates and can provide moist environment to a wound resulting in better wound healing.^{15,16} BC is a purified form of extracellular polysaccharides consisted of β -D-glucose, which is produced by several Gram-negative bacteria, such as the genera *Gluconacetobacter*, *Rhizobium*, *Agrobacterium*, *Rhodobacter* and *Sarcinau*.¹⁷ Owing to the unique physic-chemical properties of BC, including elastic properties, high tensile strength, high surface area, high porosity factor, liquid absorbing capability, biodegradability and the nano-scaled three-dimensional network structure, as well as the favorable biocompatibility, BC has been attracting increasing attention of biological medicine for wound dressing materials.¹⁸⁻²⁰ However, lacking antibacterial activity would limit its application in wound care, as bacterial infections always pose a severe threat to the wound bed.

To achieve an antimicrobial activity, different antimicrobials have been incorporated into BC such as chitosan, silver sulfadiazine, and metallic nanoparticles.^{16,21,22} Nevertheless, the toxicity of nano-silver towards mammalian cells should be taken into consideration.^{23,24} Thus, safe antibacterial agents are urgently needed. Nano-zinc oxide (nZnO) has found many applications in daily life such as in drug delivery, cosmetics, and medical devices due to its strong antimicrobial effect on a board spectrum of microorganisms.^{25,26} Moreover, it is currently listed by FDA as a generally recognized as safe (GRAS) material.²⁷ Recent studies have shown that photocatalytic bacterial-disruption and reactive oxygen species (ROS) bacterial-attack play essential roles in the antibacterial activity of nZnO.²⁸ Furthermore, zinc ion has broad potential to enhance wound healing.²⁹ Thus, nano-zinc oxide is considered as an ideal antibacterial agent for inclusion in biomaterials.

Although several methods have been used to coat BCM with nZnO, the complicated methods of preparation and

the structural features of destruction that occur during the synthetic process renders them undesirable.^{30,31} For instance, only submicron to nano-sized particles could penetrate in BCM. Penetrating materials might not be homogenously distributed inside the BCM.³² The synthesis strategy might disturb the basic structural features of BCM. In this work, carboxyl BC membrane (BCM) prepared via maleic anhydride was used as template for the in-situ assembly of nZnO/BCM bionanocomposites wound dressing. The main objective of this study is to fabricate nZnO/BCM with stable combination, select nZnO/BCM with optimal nZnO content which possesses antibacterial activity, homogenous distribution and has no cytotoxicity, and evaluate the possibility of the practical application of wound dressings to promote infected wound healing.

Materials and Methods

Materials, Cells and Animals

Lithium chloride (LiCl), N,N-Dimethylacetamide (DMAc), maleic anhydride (MA), and zinc acetic were purchased from Sigma-Aldrich. Bacteria cellulose membrane (BCM) was supplied by Hainan Guangyu Biotechnology Co., Ltd. The mouse fibroblast cell L929 was purchased from the Type Culture Collection of the Chinese Academy of Sciences, Shanghai, China. The New Zealand White rabbits and BALB/c mice were purchased from the Experimental Animal Department of the Third Military Medical University. All the animal experimental procedures had obtained the approval from the Animal Experiment Ethics Committee of the Third Military Medical University (Animal Ethical Statement). Methods employed here were carried out following the Care and Use of Laboratory Animals published by the National Institutes of Health (NIH Pub. No. 85-23, revised 1996). The animals were individually raised in plastic cages under standardized conditions (room temperature: 25°C; relative humidity: 50%; and circadian rhythm: 12 hrs). The animals were fed on autoclaved standard rodent chow and water ad libitum and were adaptively bred for 1 week in the facility before the experiments.

Fabrication of the nZnO/BCM Composites

Chemical Modification of BCM

The dehydrated BCM was soaked in the swelling solution with 5.0 (w/v) % LiCl dissolved in DMAc at room temperature for 8-12 hrs to attain an obvious swelling of the BCM. After the appropriate swelling of BCM, the solvent

was replaced by pure DMAC to stop the swelling. Then, the pulverized MA was added into the system and then the reaction was maintained at 60°C for 3 hrs under mild magnetic stirring. Following the reaction, the modified BCM was gently transferred into anhydrous ethanol to remove the unreacted chemicals. After completely washing by anhydrous ethanol, the modified BCM was either utilized to load ZnO, or fully washed by deionized water and lyophilized to obtain the intermediate product for characterization. The MA modified BCM was marked as BCM-MA. The complete route of the reactions was shown in Scheme 1.

In situ Synthesis of nZnO/BCM Composite Dressings

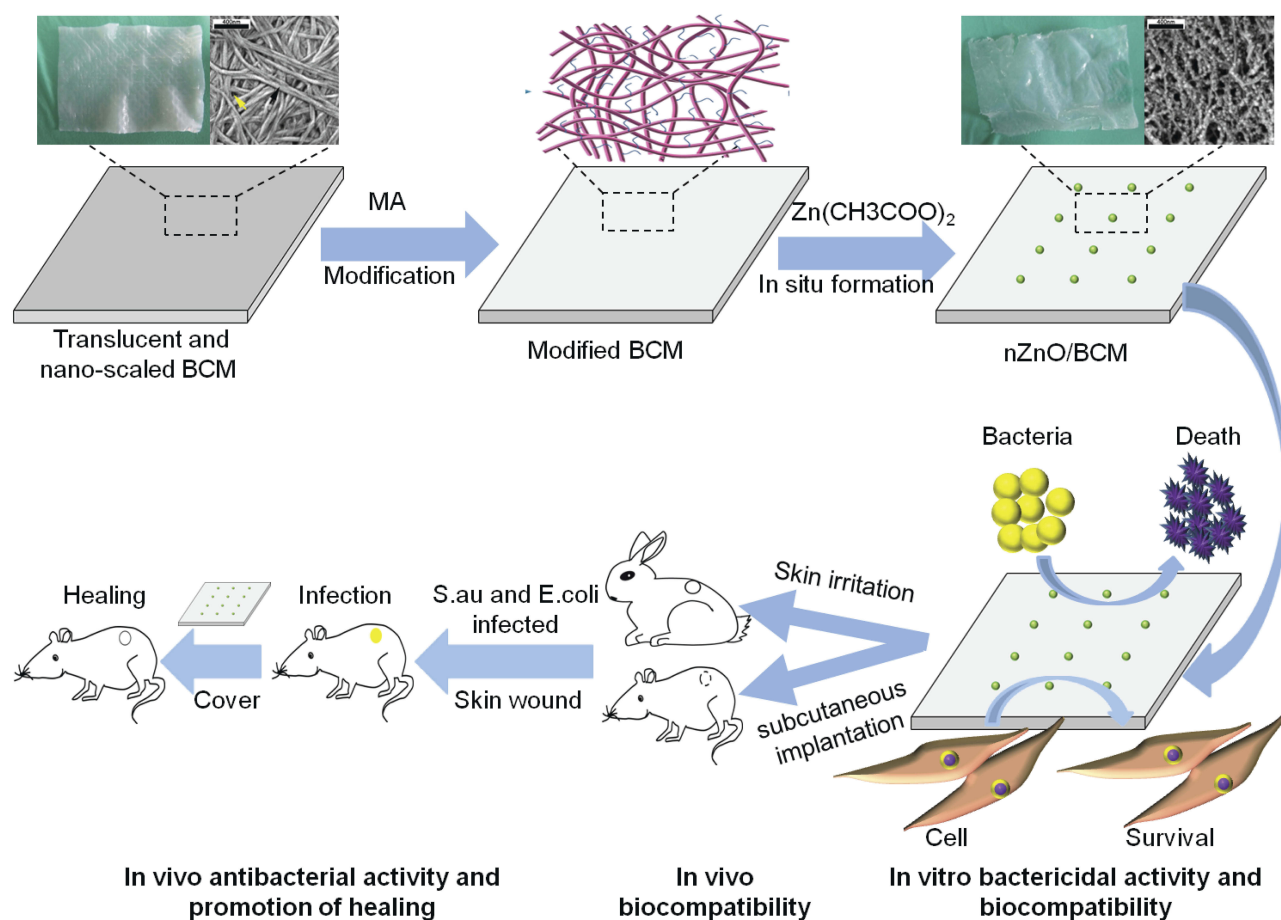
The nZnO was in situ synthesized by method using chemical modified BCM as template. The complete route of the reactions was shown in Scheme 1. Firstly, the modified BCM samples were soaked in zinc acetic solution in anhydrous ethanol with different concentrations for 1 hr at 50°C, to allow the penetration of zinc acetic into the

cellulose network. Then, anhydrous ethanol with sodium hydroxide (NaOH) dissolved at different concentrations was decanted into system. The reaction system was kept at 50°C and mild stirred for 2 hrs. Subsequently, the outcomes were completely rinsed by deionized water and freeze-dried. After the freeze-drying, the attained membranes were further dried in oven at 120°C for 1 hr. The finally prepared membranes were bacterial cellulose loaded with nZnO nanoparticles and marked as nZnO/BCM. The different final products were marked nZnO/BCM-1, nZnO/BCM-2, nZnO/BCM-3 and nZnO/BCM-4, respectively. The nZnO content of the nZnO/BCM and their main preparation conditions are shown in Table 1.

Materials Characterization

Quantification of nZnO

The quantity of nZnO contained in the nZnO/BCM was measured by using atomic absorption spectroscopy (AAS). The samples were accurately weighed and incinerated in crucibles to burn all organic contents by heating to 1100°C



Scheme 1 Schematic of the synthesis and the biological role of nZnO/BCM.

Table 1 Main Preparation Conditions of Different nZnO/BCM

Specific	nZnO Content (wt.%)	Zinc Acetic (mol/L)	Sodium Hydroxide (mol/L)
nZnO/BCM 1	5wt.%	0.01 mol/L	0.02 mol/L
nZnO/BCM 2	15wt.%	0.015 mol/L	0.04 mol/L
nZnO/BCM 3	25wt.%	0.02 mol/L	0.04 mol/L
nZnO/BCM 4	35wt.%	0.04 mol/L	0.08 mol/L

in a muffle furnace. The generated ash was then dissolved by nitric acid and diluted to constant volume. Then, the different zinc-containing solution samples were measured by Atomic Absorption Spectrometer (SpectrAA 220FS, Varian, USA). Accordingly, the nZnO contained in nZnO/BCM can be calculated.

The stability of loaded nZnO in nZnO/BCM was evaluated by two steps: autoclaving and immersing. The films were soaked in PBS and the ratio of superficial area of membrane to volume of PBS was 1.25 cm²:1mL according to the criteria in ISO 10993.12. Then, the solution with soaked membranes were sterilized by autoclave at 121°C for 30 min. The sterilized films were immersed in fresh PBS with the same volume and the extraction process was carried out at 37°C in oscillator for 24 hrs. The treated membranes were further digested by heat and measured by AAS to acquire the ZnO contents by the method mentioned above. Then, the stability of the loaded ZnO of nZnO/BCM was analyzed.

Observation of the Porous and the Cellulose Fiber Structure of the nZnO/BCM

The porous structure and surface nature of the prepared nZnO/BCM were characterized by scanning electron microscope (SEM, Hitachi S4800, Japan). Briefly, the nZnO/BCM or BCM were cut into small pieces (3 × 3mm), coated with gold-palladium under a vacuum atmosphere and then observed under an SEM.

Determination of the Water Vapor Transmission Rate (WVTR) of the Prepared Membranes

To determine the moisture permeability of the 5wt. % nZnO/BCM and BCM, the WVTRs were measured according to the American Society for Testing and Materials (ASTM) standard. A sample was cut into a disc with a diameter of 35 mm and mounted on the mouth of a cylindrical cup with a diameter of 34 mm containing 10 mL of water. The sample was sealed with Teflon tape across the edge and then placed into an

incubator kept at 37°C and 50% relative humidity. The assembly was weighed every 2 hrs for 24 hrs, and the results were recorded automatically by using the water vapor transmission rate tester (W3/030, Labthink, China). All measurements were repeated three times (n = 3).

Detection of Carboxyl Groups

The presence of carboxyl groups was detected by the Fourier transform-infrared (FT-IR) spectrum, and samples were recorded using a Thermo Nicolet Avatar 360 FT-IR Spectrometer. The intact BC and lyophilized BC-MA films were tested directly by ATR FT-IR. They were scanned from 600 cm⁻¹ to 4000 cm⁻¹ with a resolution of 2 cm⁻¹ by using Thermo Fisher Nicolet IS10 (USA).

Measurement of the Mechanical Properties of the Membranes

The mechanical properties of the BCM and the nZnO/BCM were measured by tensile testing. Briefly, Samples were cut into a dumbbell shape and tested by the Q800 materials testing system (TA, USA). The samples were clamped, oriented vertically and stretched to failure. The velocity of stretching was 50µm/min, and the results were recorded automatically. Three specimens were tested for each group (n=3).

Cytotoxicity Test

Cytotoxicity of the membranes with different content of nZnO was evaluated by indirect cytotoxicity test using MTT assay according to ISO 10993–12 protocols. The membranes were sterilized by autoclave beforehand. The sterilized membranes were immersed in Dulbecco's Modified Eagle's Medium (DMEM) containing 10% fetal bovine serum (FBS) and placed at 37°C for 24 hrs to produce extraction media. Fresh DMEM supplemented with 10% FBS was used as a control. L929 Mouse fibroblasts were plated in 100µL of DMEM supplemented with 10% FBS at a density of 1 × 10⁴ cells/well in 96-well plates, and the cells were cultured at 37°C in a wet atmosphere containing 5% CO₂. The medium was replaced by the extraction medium after 24 hrs, and the cells were incubated for an additional 24 hrs. The tested extraction solutions were then removed. Finally, the cells were incubated in 100µL of MTT-containing medium (1 mg/mL) for 4 hrs. After the medium was removed, the formazan crystals formed in the living cells were dissolved in 100µL of dimethyl sulfoxide. Relative growth rate (%) of the cells compared to control was calculated based on the

absorbance at 570 nm using a multifunctional microplate reader (Thermo Scientific Varioskan).

Evaluation of in vitro Antibacterial Activity of the nZnO/BCM

The antibacterial activity was evaluated against gram-positive *S. aureus* and Gram-negative *E. coli*. The strains were cultured in LB broth overnight at 37°C in a shaking incubator, and then transferred to fresh and sterile flask containing LB broth at a concentration of 1×10^6 colony forming unit per milliliter (CFU/mL). The nZnO/BCM pieces (33mg, 1×1 cm) sterilized by autoclave were added to the tubes and kept for incubation at 37°C for 24 hrs. The intact BCM was taken as a negative control. After the specified time period, LB broth containing the bacteria were serially diluted in sterile saline and plated on LB agar plates. The number of bacterial colonies were counted and plotted to quantify the antibacterial activity.

Skin Irritation Test

The primary skin irritation test was performed on healthy New Zealand White rabbits (weighing 2–2.5 kg). The rabbits were randomly divided into two groups, i.e. a single application group and a multiple application group. The fur was removed from the dorsal surface of the rabbits 24 hrs prior to administration. For the irritation test, the dorsal skin of each rabbit was divided into eight regions for the application of the gauze immersed with normal saline (NS), BCM, the 5wt.% nZnO/BCM, and the gauze immersed with 20%-sodium lauryl sulfate (20%SLS). For the single application group, the samples were applied to the corresponding regions, and the rabbits were examined for signs of irritation at 1, 24, 48, and 72 hrs after application. For the multiple application group, the samples were applied to the same skin regions for 24 hrs. The application sites were assessed 1 hr after removal of the samples, and the same procedure was repeated for another 6 days. After the final removal, the samples in the multiple administration group were monitored for 72 hrs. Mean erythema and edema scores were recorded according to the Draize method, i.e. for erythema and eschar formation (no erythema = 0; very slight erythema = 1; well-defined erythema = 2; moderate to severe erythema = 3; severe erythema and slight eschar formation = 4), and edema formation (no edema = 0; very slight edema = 1; slight edema = 2; moderate edema = 3; severe edema = 4). Eventually, the total scores for the irritation test in each condition are calculated using equation 2.

$$\text{Average irritation scores} = \frac{\text{erythema reaction scores} + \text{dropsy reaction scores}}{\text{amount of assessment}} \quad (1)$$

Histocompatibility Examination

BALB/c mice (n=18) were randomly divided into three groups, and the mice were under anesthesia with 1% pentobarbital via intraperitoneal injection (0.01 mg/g of body weight). The dorsal surface of the BALB/c mice was shaved and disinfected with 75% alcohol. Afterwards, 1.5 cm-sized linear wounds were made on the backs of each mouse. In the implanted group, a piece of sterilized 10 mm×10 mm nZnO/BCM or BCM was implanted subcutaneously, and the wounds were sutured with Nylon 4–0, whereas in the sham-operated group, the wounds were sutured without implanting samples.

On weeks 1, 3 and 9 after operation, samples of the tissue around the incision site were obtained by euthanizing three mice from each group. Then, the skin tissues were fixed in 4% paraformaldehyde. Six micrometer thick sections were cut and stained with haematoxylin and eosin. Light microscopy-based histological evaluation of the stained sections was performed by a pathologist blinded to the previous treatments.

In vivo Infected Wound Healing Evaluation

In vivo Antibacterial Activity Evaluation

To understand the in vivo antibacterial activity of the nZnO/BCM, the wounds with different dressings were picked off at day 3 and day 7 post wounding. Sterile glass homogenates were used to mill the tissues, which were then washed with saline. The homogenates were diluted 100-fold, and 100µL was removed and placed on Columbia blood plate medium. Subsequently, the colony forming units were conducted for each sample after incubation for 24 hrs at 37°C. Then, the following calculation was used: number of bacteria colonies/g = (number of bacterial colonies × dilution ratio/0.01)/weight of tissue.

Wound Healing Experiment

BALB/c mice were under anesthesia with 1% pentobarbital via intraperitoneal injection (0.01 mg/g of body weight). The dorsal surface of the BALB/c mice was shaved and disinfected with alcohol. A circular full-thickness defect wound (diameter 6 mm) was prepared by excising the dorsum of the mouse using a puncher. The wounds were immediately photographed

using a digital camera. The wounds were divided into four groups. In wounds covered with gauze, BCM and 5wt. % nZnO/BCM groups, 20 μ L mixed bacteria suspension in phosphate-buffer saline (PBS; PH 7.4), containing 5×10^7 CFU of *S. aureus* and the same amount of *E. coli*, was instilled into the center of each wound. A piece of sterilized 10 \times 10 mm gauze, BCM or 5wt.%nZnO/BCM was soaked in PBS and then applied on the wounds. Wounds, treated with 20 μ L PBS and gauze, were distinguished as the control group. After that, all the dressings were fixed with adhesive wound dressing (3M health care). The dressing was changed on days 3, 5, 7, 10, 12, and 14 post-surgery. To find the status of the inflammatory reaction, the wounds were soaked using PBS, and the scabs were removed gently. Meanwhile, the wounds were photographed. The initial or left areas of the wounds were measured with IPP 6.0 software based on the pictures. With the use of IPP 6.0 software, the margin of each wound was carefully traced, and the number of pixels encompassing each wound tracing was calculated. The number of pixels was then converted into square centimeters, after which the amount of residual wound was calculated by:

$$\text{Wound area (\%)} = \text{AW}_n / \text{AW}_i \times 100$$

where AW_i represented the area of the initial wound and AW_n was the area of the wound on the n th day post-surgery.

Eight mice in each group were used to determine the approximate time of wound closure.

Histological Examinations

To identify more detailed histopathological changes, at 3 and 7 days after surgery, mice were sacrificed, and their wound tissues were carefully biopsied, fixed with 4% formaldehyde, embedded in paraffin, sectioned at a thickness of 5 μ m and stained with H&E for histological analysis. The number of infiltrated inflammatory cells in granulation tissues (cells/mm² of field) was recorded. The length of the newly formed epithelium and the granulation thickness were determined with IPP 6.0 software. The measurement procedures were performed by two blind pathologists. The length of the newly formed epithelium, i.e. the length of the epithelial tongue, was defined as the distance that between the advancing edges of the epidermal keratinocytes and the presence of hair follicles in non-wounded skin. Nine sections from three mice of each group at each time-point were analyzed.

Statistical Analysis

All data were presented as the mean \pm standard error of mean (SEM). One-way ANOVA was used to evaluate

statistical significance, followed by post-hoc LSD test and Bonferroni's test. p values less than 0.05 were considered significant.

Results and Discussion

Morphology and Mechanical Properties of nZnO/BCM Nanocomposites

Morphological characterization of BCM and nZnO/BCM was determined by SEM. The results were shown in Figure 1A and B, the fibers in the intact BCM were closed to each other forming a network with small and limited pores. However, the pore size and porosity were increased in the fiber network of the nZnO/BCM. The sphere-shaped and nano-scale nZnO were closely attached and uniformly distributed in the network of bacterial cellulose, forming a unique string-beaded morphology. The pore size and porosity of the nZnO/BCM were increased compared with intact BCM, which enhanced water vapor permeability. An adequate WVTR (water vapor transmission rate) is an important parameter for wound dressing. An excessively high WVTR accelerates the dehydration and scabbing of a wound, whereas an excessively low WVTR causes wound fluids to accumulate, and impedes healing, and raises the risk of bacterial contamination. A desirable WVTR of wound dressing is 2500 ~ 3000 g/m²/day.³³ As shown in Figure 1C, the average WVTR of the nZnO/BCM was 2856.60 g/m²/day, which was significantly higher than the intact BCM (2506.56 g/m²/day). A moist environment has been believed to accelerate wound healing by enhancing cell migration.^{34,35}

The composites (BCM-nZnO), which was fabricated by taking unmodified BCM as template, were used for comparison. It was found that more than 50% of the nZnO were released in the unmodified BCM after extraction, whereas less than 10% of them were released in the modified BCM after extraction (Figure 1D). These results indicated that the modification significantly increased the binding stability of nZnO to BCM.

The chemical structures of the prepared membranes were determined using ATR-FTIR analysis. As shown in Figure 1E, the peak at 1059 cm⁻¹ arises from C–O–C pyranose ring skeletal vibration of cellulose. Compared with BCM, the FTIR spectra of BCM-MA exhibit a strong peak at 1712 cm⁻¹, which is due to C=O stretching vibrations of carboxyl groups and ester groups. Besides, the band at 1611 cm⁻¹ of the FTIR spectra of BCM-MA corresponds to C=C deformation vibration of

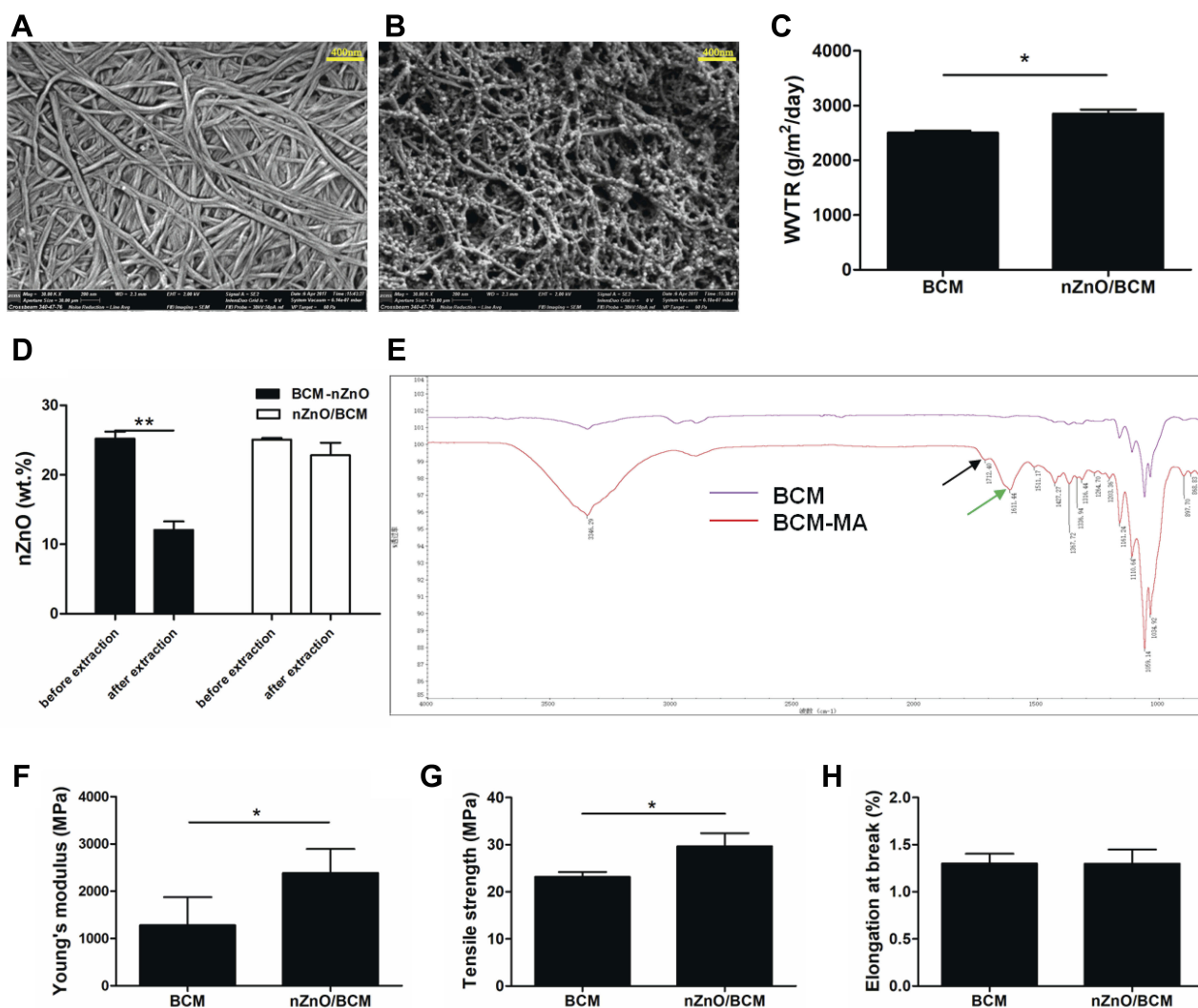


Figure 1 Morphology and mechanical properties of nZnO/BCM nanocomposites. SEM of (A) BCM and (B) nZnO/BCM. (C) WVTR of as-prepared membranes. (D) Stability evaluation of nZnO/BCM. (E) FTIR spectra. Mechanical properties of as-prepared membranes: (F) Young's modulus, (G) Tensile strength, (H) Elongation at break and. * $p < 0.05$, compared to BCM. ** $p < 0.01$, compared to unmodified BCM before extraction. Data were presented as mean \pm SEM ($n = 3$).

vinyl groups, which is not detected on The FTIR spectra of BCM. C=O stretching vibrations and C=C deformation vibration confirm the presence of carboxyl groups, suggesting the success of the proposed modification.

An ideal wound dressing should possess excellent flexibility and mechanical strength so that it can protect wounds from physical damage and resist deformation caused by rubbing or collision.^{36,37} Therefore, tensile testing was used to determine the mechanical properties of nZnO/BCM. As shown in Figure 1F, the Young's modulus of the nZnO/BCM was 2387.41 MPa which was nearly double of the intact BCM, namely, 1280.28 MPa. The average tensile strength of the nZnO/BCM was 29.68 MPa, which was significantly higher than that of the intact BCM (23.17 MPa) (Figure 1G). Elongation at break of the

nZnO/BCM was approximate 1.30%, which was similar to the intact BCM (Figure 1H). nZnO/BCM nanocomposite membranes exhibited a higher tensile strength and percent elongation at break and lower Young's modulus, indicating that our nanocomposites were flexible, comfortable and resilient.³⁸ Collectively, the synthesized nZnO/BCM composite membranes with excellent mechanical performances could be valuable candidates for wound dressings.

5wt. % nZnO/BCM Exhibited Antibacterial Activity with Non-cytotoxicity

Biosafety is a crucial factor for a wound dressing; therefore, we meticulously investigated the cytotoxicity of nZnO/BCM membranes by MTT assay, and the results were summarized in Figure 2. According to ISO 10993-12 protocols, the 5wt. %

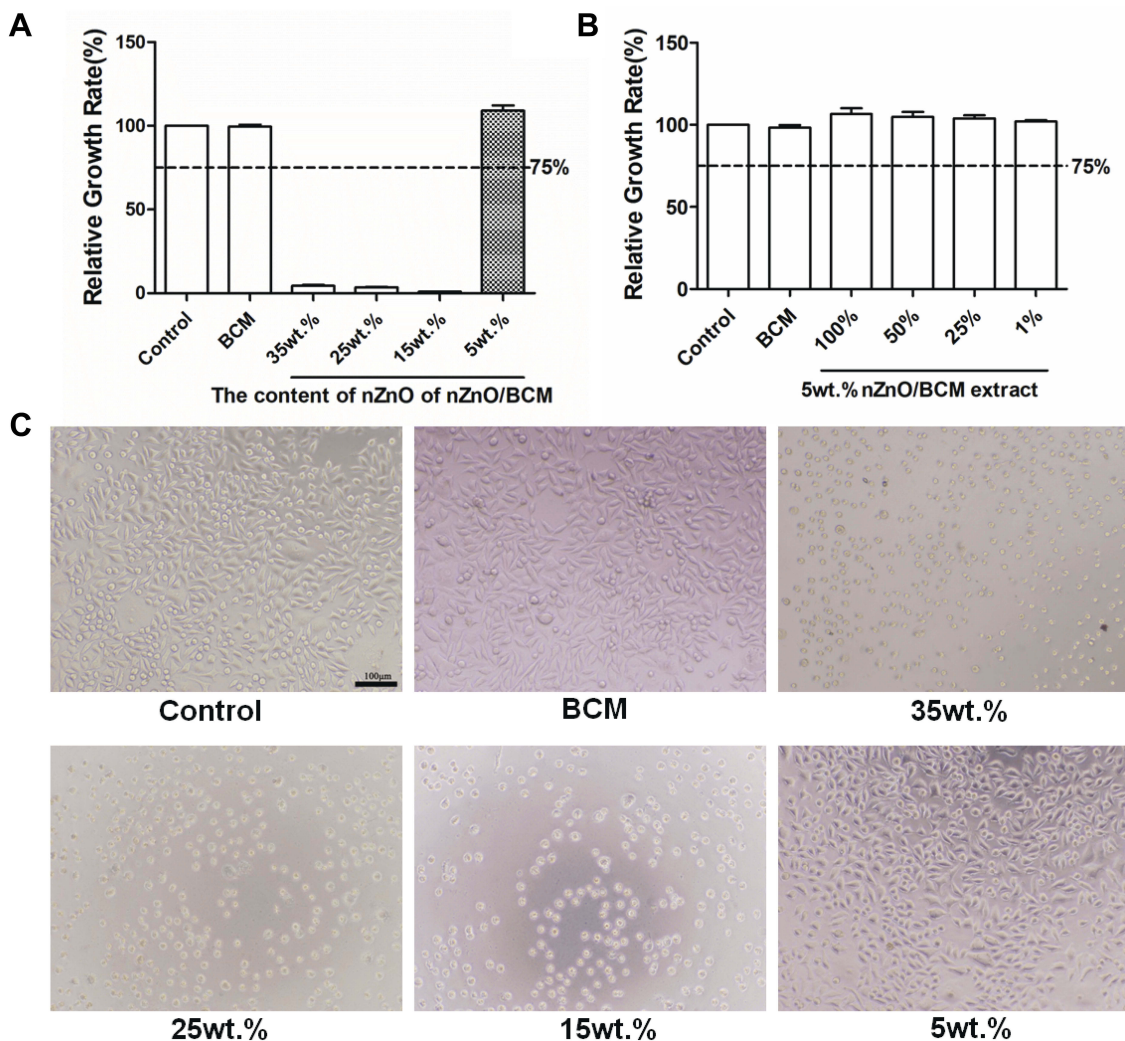


Figure 2 Cytotoxicity evaluation of membranes. (A) Different concentrations of nZnO cytotoxicity evaluation. (B) Leaching solution of 5wt.% nZnO/BCM cytotoxicity evaluation. (C) Corresponding cell morphology of fibroblasts after 48 hrs. Data were presented as mean±SEM (n=5).

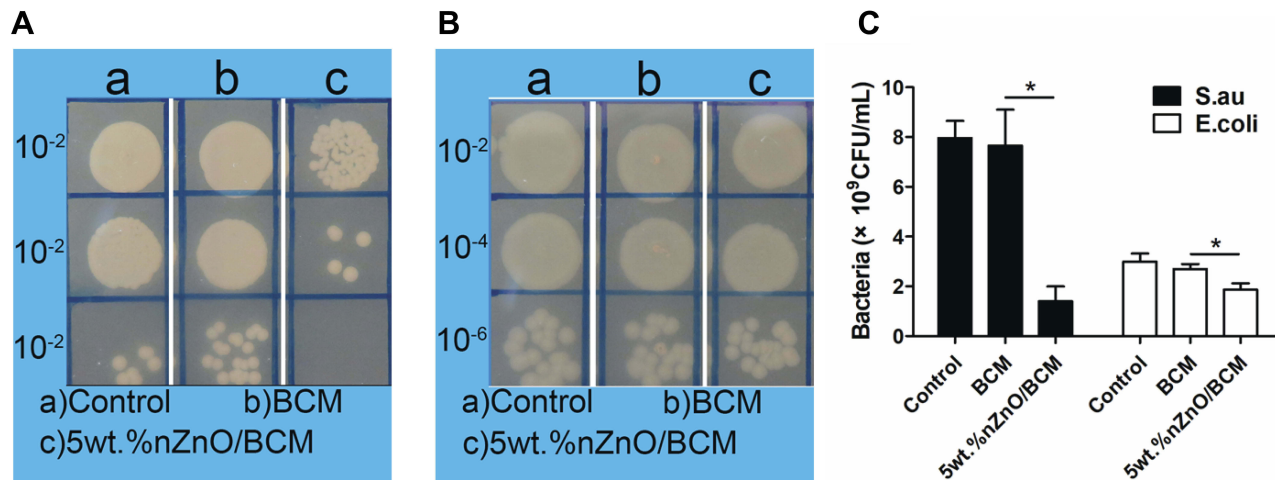


Figure 3 Antibacterial activity of the 5wt.% nZnO/BM was tested against (A) *S. aureus* and (B) *E. coli* by serial dilution method. The label on y-axis shows dilution factor. (C) The concentration of bacteria suspension after incubation for 24 hrs with different dressings. *p<0.05, compared to BCM. Data were presented as mean±SEM (n=4).

Table 2 Average Response Scores of Skin Irritation for Single Application (n = 6)

Samples	Average Score			
	1 hr	24 hrs	48 hrs	72 hrs
NS	0	0	0	0
BCM	0.33	0.33	0	0
5wt.% nZnO/BCM	0.17	0.17	0	0
20% SLS	4	8	8	8

Table 3 Average Response Scores of Skin Irritation for Multiple Application (n = 6)

Samples	Average Score			
	1 hr	24 hrs	48 hrs	72 hrs
NS	0	0	0	0
BCM	0.17	0	0	0
5wt.%nZnO/BCM	0.33	0.33	0	0
20%SLS	8	8	8	8

nZnO/BCM exhibited no cytotoxicity to mouse fibroblast cells, which was similar to the intact BCM. By contrast, the composites with 35wt. %, 25wt. % and 15wt. % showed drastic cytotoxicity. Therefore, adsorption of nZnO/BC bionanocomposites should be taken into consideration. It is reported that the introduction of carboxyl groups to cellulose via anhydride shows significant increase in the adsorption capacity of Cu, Cd, and Pb.³⁹ In this work, carboxyl BC membrane (BCM) prepared via maleic anhydride was used as template

for the in-situ assembly of nZnO/BCM bionanocomposites wound dressing.

According to the consequence mentioned above, the 5wt. % nZnO/BCM was used for the following tests. We measured the antibacterial activity of the 5wt. % nZnO/BCM against *S. aureus* and *E. coli* in vitro using shaking flask method. As shown in Figure 3A and B, serial dilution of bacteria was indicated from top to bottom and the different samples were indicated from left to right. It was clear that the number of bacterial colonies was significantly decreased in the presence of the 5wt. % nZnO/BCM. The bacteriostatic rate of the 5wt. % nZnO/BCM was 78.64% and 37.67% to *S.aureus* and *E. coli*, respectively (Figure 3C). These results demonstrated that nZnO/BCM nanocomposites could efficiently inhibit bacterial growth. By contrast, BCM did not show any antibacterial activity against both *S. aureus* and *E. coli* compared with control. To achieve an antimicrobial activity, different antimicrobials have been incorporated into BC such as chitosan, octenidine, silver sulfadiazine, and metallic nanoparticles.^{16,21,40,41} Recent studies have shown that nZnO has effective antibacterial activity towards gram-positive and gram-negative bacteria. The antibacterial mechanism including the release of antimicrobial ions, interaction of nanoparticles with microorganisms, subsequently damaging the integrity of bacterial cells and the formation of reactive oxygen species (ROS) by the effect of light radiation. Among these factors, photocatalytic bacterial-disruption and reactive oxygen species (ROS)

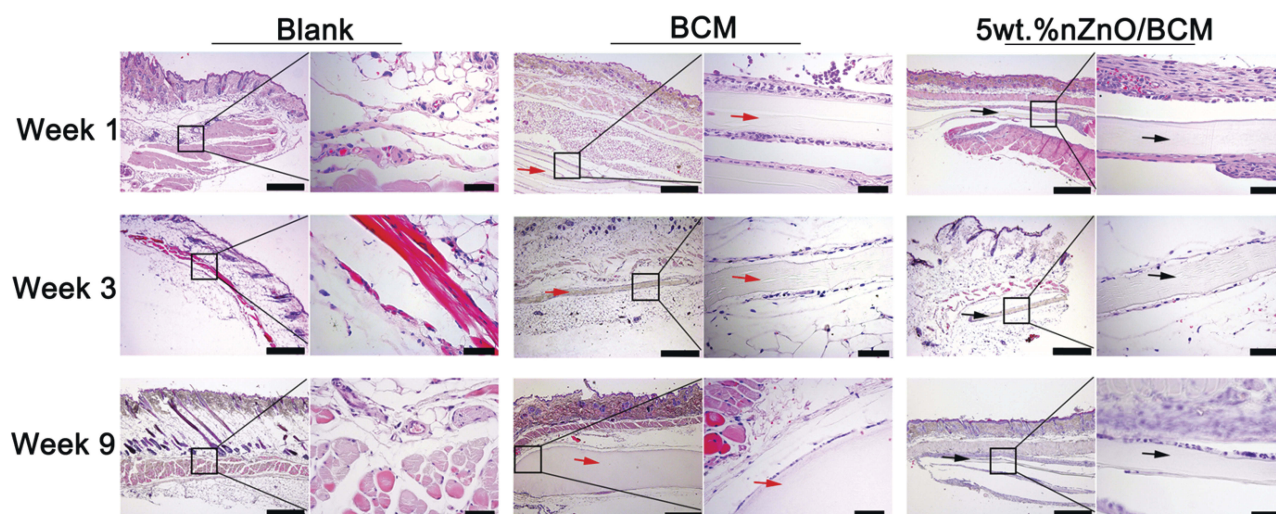


Figure 4 H&E stained images of the tissue containing the implanted BCM and 5wt.%nZnO/BCM. No signs of inflammation were observed around the samples on weeks 1, 3 and 9 after the operation. In the control group, no sample was implanted, whereas the BCM and 5wt.% nZnO/BCM groups underwent implantation of the corresponding samples. The scale bars in the prior column indicate 500 μ m and those in the posterior column indicate 50 μ m. The red arrows indicate the implanted BCM, and the black arrows indicate the implanted 5wt.% nZnO/BCM.

bacterial-attack play essential roles in the antibacterial activity of nZnO.²⁸ While antibacterial activities of this composite against *S. aureus* were stronger than *E. coli*. The outer membrane of Gram-negative bacteria acts as a permeability barrier, so that the absorption of ROS into the cell is reduced. Similar results on the antibacterial activity of ZnO been reported by other researchers.^{42,43} The main objective of this study is to fabricate nZnO/BCM with stable combination, select nZnO/BCM with optimal nZnO content which possesses antibacterial activity and has no cytotoxicity.

The 5wt. % nZnO/BCM Was Nonirritant to the Skin

Skin irritation tests were performed on the dorsal skin of the healthy New Zealand White rabbits. The quantitative

data were summarized in Tables 2 and 3. Total scores below 0.5 were considered as nonirritant. 5wt. % nZnO/BCM, the intact BCM or the gauze caused no irritation to normal skin at all the observed time points after a single application or multiple applications, whereas 20% SLS, a positive control, showed an obvious skin irritation with the crust formation. These results indicated that the 5wt. % nZnO/BCM had no stimulation to skin and was acceptable as a wound dressing.

Histocompatibilities of the 5wt. % nZnO/BCM

Histocompatibility of the 5wt. % nZnO/BCM was determined by implantation experiment in vivo using BALB/c mice. On the week of 1, 3 and 9 postimplantation, tissues containing implants were obtained, respectively, and then

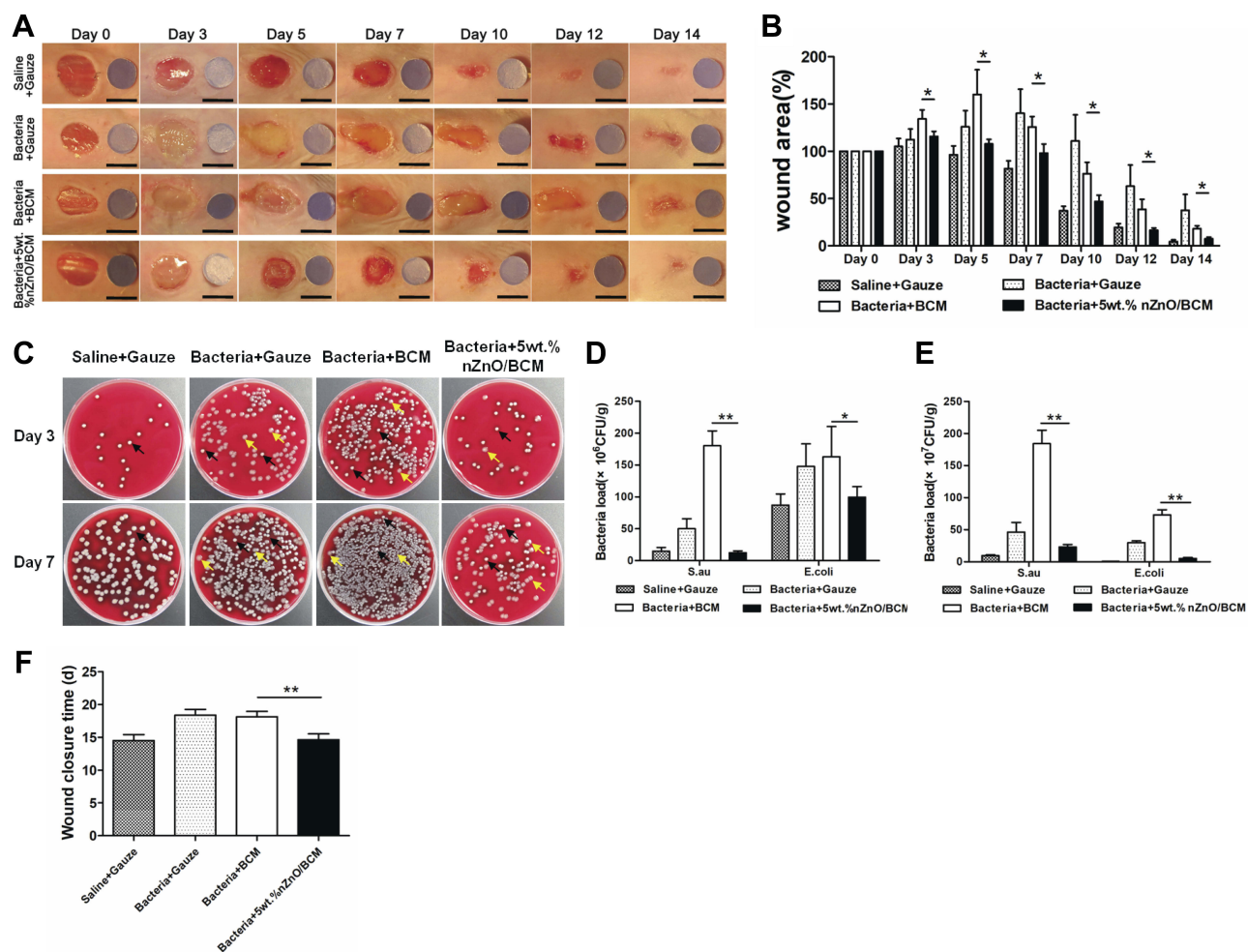


Figure 5 The effect of 5wt.%nZnO/BCM on the healing of bacteria-infected wounds. (A) The macroscopic appearance of wounds from blank, saline gauze, BCM and 5wt.%nZnO/BCM groups. (B) The percentage of residual wound areas at days 3, 5, 7, 10, 12 and 14 post-surgery. (C) Photographs and (D) and (E) quantitative counts of bacterial colonies formed by *S. aureus* and *E. coli* obtained from wound tissues. The black arrows represent the colony of Gram-positive *S. aureus*; the yellow arrows indicate the colony of Gram-negative *E. coli*. (F) Average days for wound closure. * $p < 0.05$, ** $p < 0.01$, compared to bacteria+BCM group. Data were presented as mean \pm SEM ($n=4$). The scale bars indicate 6 mm.

observed histologically. As shown in Figure 4 no degradation of the implants was observed in all the groups at all the indicated time points. The implants were surrounded by a tissue capsule that consisted of fibroblasts and collagen, and the thickness of the tissue capsule turned to thinner as the time passed. Little infiltration of the inflammatory cells could be found in the tissues around the implanted 5wt. % nZnO/BCM as well as BCM, which indicated that nZnO/BCM had acceptable biocompatibility in vivo.

The Effect of nZnO/BCM on the Healing of Bacteria-Infected Wounds

Wound healing process was shown as Figure 5A. There was no sign of wound infection in normal wounds covered with gauze during the healing process. However, an obvious inflammatory reaction was found on day 3 post-wounding

in all the wounds administrated with *S. aureus* and *E. coli*: pus substances were observed on the wound bed, the skin around the wounds was inflamed, and the wound size seemed to be larger than that of day 0 post-wounding. This confirmed that the infected wound model was successfully fabricated in mice. The wound inflammation got more serious, as indicated by the enlargement of wound size, on day 5 or day 7 post-wounding in gauze and BCM groups and did not disappear until day 10 or 12 post-wounding in those mice. By contrast, the inflammation in 5wt. % nZnO/BCM group subsidized since day 5 post-wounding and wounds covered with 5wt. % nZnO/BCM seemed to be neat and moist with the fresh granulations generated on the wound bed, and the newly formed epidermis could be clearly observed at the margin of the wounds since day 5 and up to day 14 post-wounding. The quantitative data for the closed wound area also supported these results. The

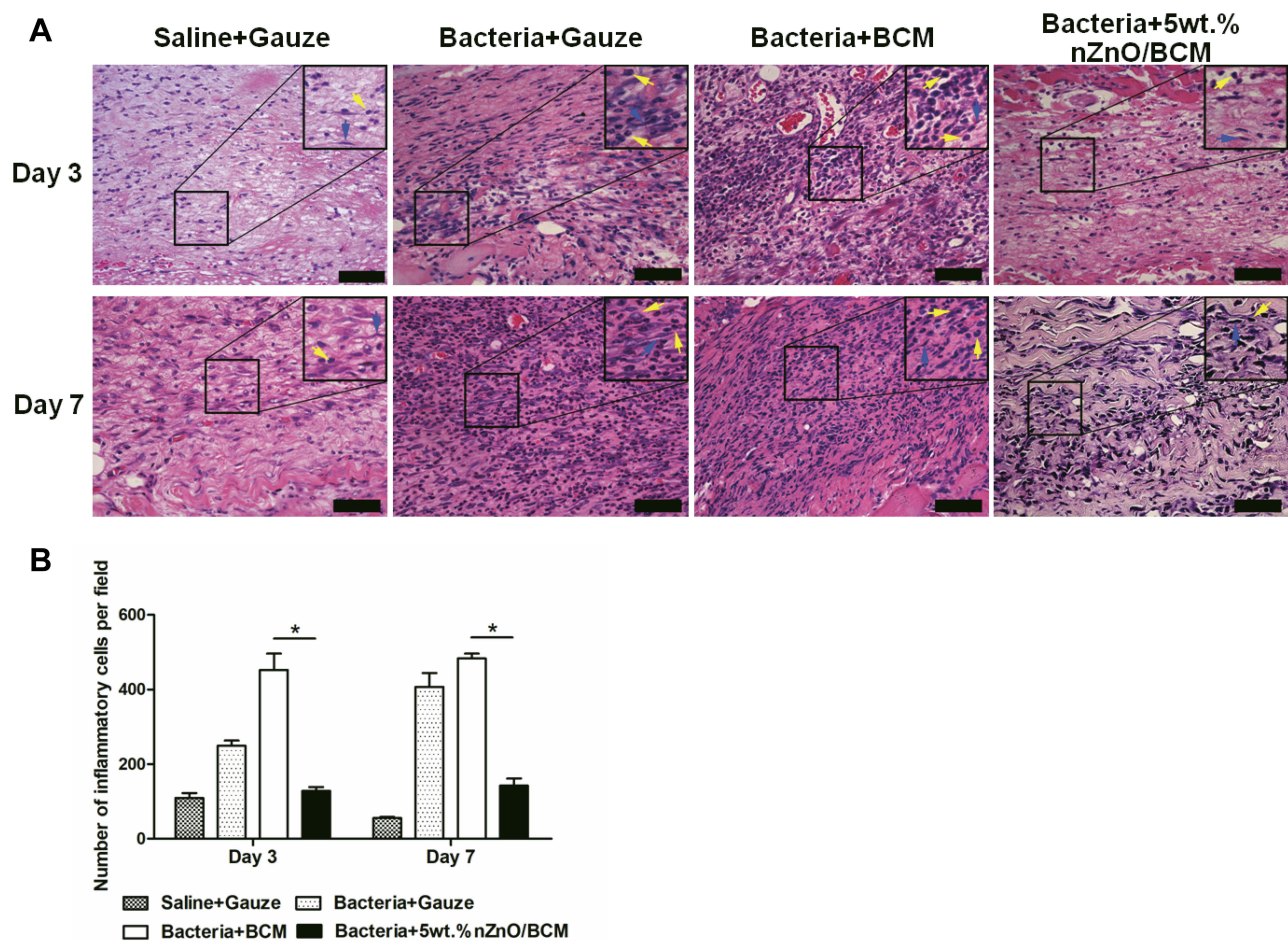


Figure 6 The effect of 5wt.%nZnO/BCM on inflammation. **(A)** Representative H&E staining images of blank, saline gauze, BCM and 5wt.%nZnO/BCM groups at days 3, and 7 post-surgery. The blue arrows represent fibroblasts; the yellow arrows indicate inflammatory cells. **(B)** Quantitative counts of inflammatory cells infiltrated in the wound region of *S. aureus* -infected wounds and *E. coli* -infected wounds. *p<0.05, compared to bacteria+BCM group. Data were presented as mean±SEM (n=5). The scale bars indicate 50 μm.

healing process of the infected wounds covered with 5wt. % nZnO/BCM was significantly improved compared with that of the infected wounds covered with gauze or BCM. On the 14th day, area of the infected wounds covered with 5wt. % nZnO/BCM approximately was 7.5%, which was significantly smaller than that of the infected wounds covered with BCM and gauze (37.5% and 17.8%, respectively, $p < 0.05$, Figure 5B). And other similar kinds of situations were observed on days 3, 5, 7, 10 and 12 post-wounding.

Simultaneously, to evaluate the actual bactericidal effect of nZnO/BCM in vivo, wound bacteria were isolated and quantified using a method of biopsy homogenate. It was found that the numbers of bacteria colonies were significantly decreased in the infected wounds covered with 5wt. % nZnO/BCM, compared with those covered with gauze or BCM on day 3 or day 7 post-wounding (Figure 5C–E). These results demonstrated a strong and persistent activity of 5wt. % nZnO/BCM against *S. aureus* and *E. coli* in vivo.

Additionally, we found that application of nZnO/BCM membranes significantly shortened the wound closure time. As shown in Figure 5F, the average closure time was 14.6 days in the infected wounds covered with 5wt. % nZnO/BCM, whereas it was 18.1 days and 18.4 days in the infected wounds covered with gauze and BCM, respectively ($P < 0.01$).

Taken together, these data indicated that nZnO/BCM could efficiently eliminate *S. aureus* and *E. coli* infections in vivo, leading to rapid wound healing.

Infiltration of Inflammatory Cells Were Reduced by 5wt. % nZnO/BCM Treatment

Infiltration of inflammatory cells is a maker of wound bacterial infection; thus the inflammatory cells were quantified in all the wounds by H&E staining of tissue sections. As shown in Figure 6A, an obviously increased infiltration of inflammatory

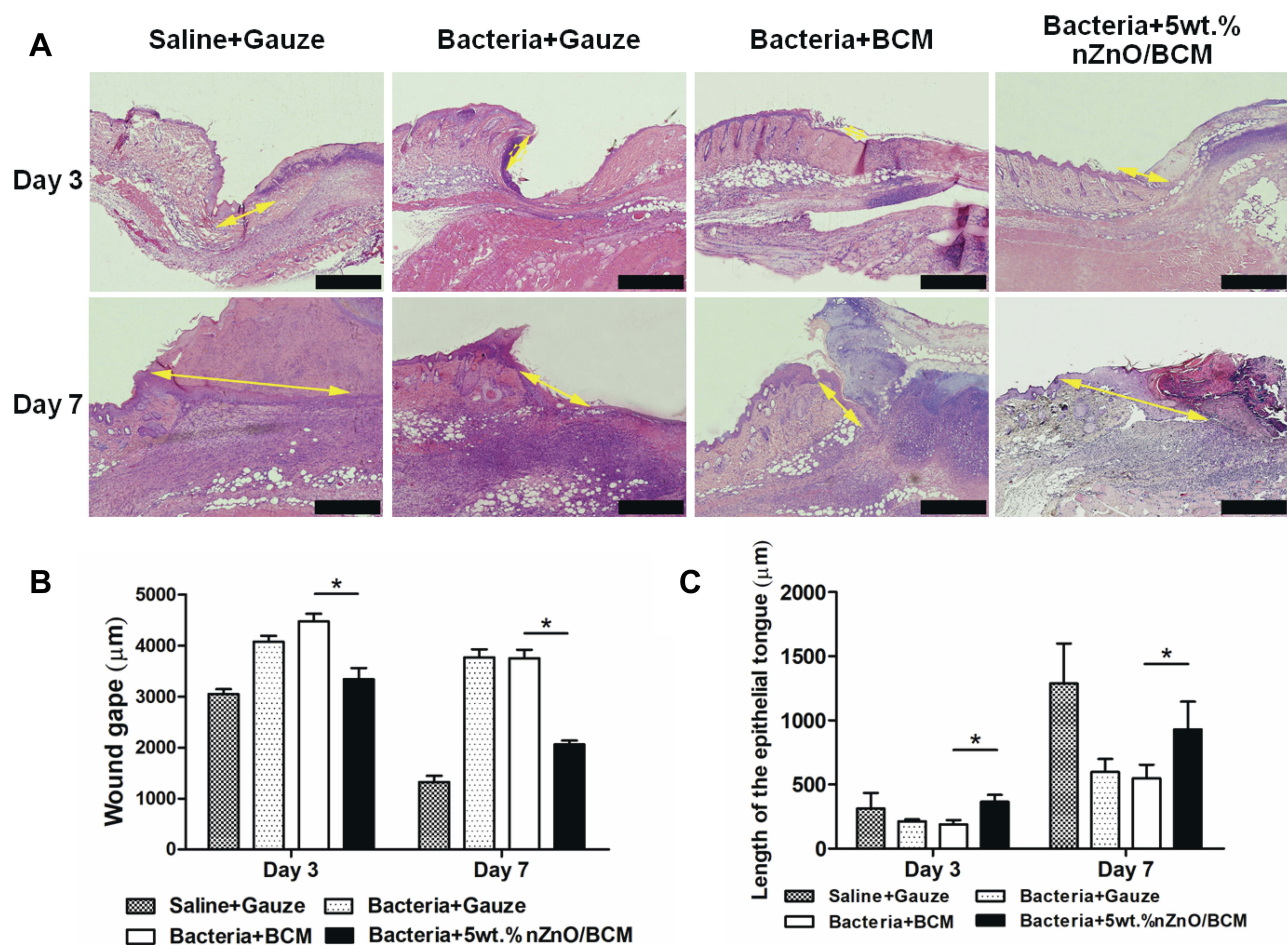


Figure 7 The effect of the 5wt.%nZnO/BCM on re-epithelialization and wound contraction: (A) Representative H&E staining images of wounds. The arrows indicate the newly formed epithelium. (B) Mean wound gap. (C) Length of newly formed epithelial tongue. * $p < 0.05$, compared to bacteria+BCM group. Data were presented as mean \pm SEM (n=5). The scale bars indicate 500 μ m.

cells was observed on day 3 and day 7 post-wounding in gauze and BCM group, but not 5wt. % nZnO/BCM treated infected wounds when compared with non-infected wound controls. Quantitative analysis showed that the amount of inflammatory cells in wounds treated with 5wt. % nZnO/BCM on day 3 and day 7 were 128.1 and 142.4 (Figure 6B), which was smaller than those of the infected wounds treated with gauze (day 3: 249.3, day 7: 407.2, respectively) and BCM (day 3: 452.1, day 7: 483.1, respectively). These results further indicate that treatment with nZnO/BCM can effectively prevent bacterial infections and maintain a natural microenvironment for tissue regeneration.

Both Wound Contraction and Wound Reepithelialization Were Enhanced by 5wt. % nZnO/BCM

We determined the amount of wound contraction in the mouse wound healing model. On day 3 post-wounding, the amount of wound contraction was similar in all the infected wounds, which were all significantly smaller than that of the non-infected wound covered with gauze (Figure 7A–B). However, on day 7, the amount of wound contraction in 5wt. % nZnO/BCM group was significantly higher than those treated by gauze and BCM, respectively.

We measured the length of the newly formed epithelium in all the wounds based on the H&E staining sections. It was found that the length of newly regenerated epidermis in 5wt. % nZnO/BCM group was significantly longer than those covered with gauze and BCM on day 3 and day 7 post-wounding (Figure 7C). These results indicated that the nZnO/BCM was able to promote wound closure by accelerating the re-epithelialization and wound contraction in the infected wounds. More importantly, rapid re-epithelialization is conducive to reduce hypertrophic scar formation.

Conclusions

We developed a new type of composite membrane consisting of BC and nZnO by modification of BC and situ synthesis of nZnO. The selected 5wt. % nZnO/BCM with well stability achieved network structure with high porosity, good physical properties, appropriate water vapor permeability, nontoxicity, antibacterial activity and good biocompatibility, and maintain a nonseptic and normal wound microenvironment for tissue regeneration, leading to rapid re-epithelialization and wound closure, while causing no measurable damage to normal tissues. Therefore, the

constructed nZnO/BCM has great potential for biomedical applications such as wound management.

Acknowledgments

This work was supported by National Nature Science Foundation of China (NSFC No. 81571900) and the Promotion Project for Application Technology Research and Demonstration of Hainan Province of China (ZDXM2014089).

Author Contributions

All authors contributed to data analysis, drafting or revising the article, gave final approval of the version to be published, and agree to be accountable for all aspects of the work.

Disclosure

Prof. Dr. Hai Lin reports a patent for the preparation and application of bacterial cellulose wound dressing with anti-bacterial property licensed to 201510301459X. The authors report no other conflicts of interest in this work.

References

- Aljghami ME, Saboor S, Amini-Nik S. Emerging innovative wound dressings. *Ann Biomed Eng.* 2019;47(3):659–675. doi:10.1007/s10439-018-02186-w
- Mogosanu GD, Grumezescu AM. Natural and synthetic polymers for wounds and burns dressing. *Int J Pharm.* 2014;463(2):127–136. doi:10.1016/j.ijpharm.2013.12.015
- Branco da Cunha C, Klumpers DD, Li WA, et al. Influence of the stiffness of three-dimensional alginate/collagen-I interpenetrating networks on fibroblast biology. *Biomaterials.* 2014;35(32):8927–8936. doi:10.1016/j.biomaterials.2014.06.047
- Andrews KL, Houdek MT, Kiemle LJ. Wound management of chronic diabetic foot ulcers: from the basics to regenerative medicine. *Prosthet Orthot Int.* 2015;39(1):29–39. doi:10.1177/0309364614534296
- P TS, Lakshmanan VK, Raj M, et al. Evaluation of wound healing potential of beta-chitin hydrogel/nano zinc oxide composite bandage. *Pharm Res.* 2013;30(2):523–537. doi:10.1007/s11095-012-0898-y
- Lv D, Wang R, Tang G, et al. Ecofriendly electrospun membranes loaded with visible-light-responding nanoparticles for multifunctional usages: highly efficient air filtration, dye scavenging, and bactericidal activity. *ACS Appl Mater Interfaces.* 2019;11(13):12880–12889. doi:10.1021/acsami.9b01508
- Ding Q, Xu X, Yue Y, et al. Nanocellulose-mediated electroconductive self-healing hydrogels with high strength, plasticity, viscoelasticity, stretchability, and biocompatibility toward multifunctional applications. *ACS Appl Mater Interfaces.* 2018;10(33):27987–28002.
- Matsumura H, Imai R, Ahmatjan N, et al. Removal of adhesive wound dressing and its effects on the stratum corneum of the skin: comparison of eight different adhesive wound dressings. *Int Wound J.* 2014;11(1):50–54. doi:10.1111/iwj.2014.11.issue-1
- Sood A, Granick MS, Tomaselli NL. Wound dressings and comparative effectiveness data. *Advan Wound Care.* 2014;3(8):511–529. doi:10.1089/wound.2012.0401

10. Dhivya S, Padma VV, Santhini E. Wound dressings - a review. *Biomedicine (Taipei)*. 2015;5(4):22. doi:10.7603/s40681-015-0022-9
11. Fu SZ, Meng XH, Fan J, et al. Acceleration of dermal wound healing by using electrospun curcumin-loaded poly(epsilon-caprolactone)-poly(ethylene glycol)-poly(epsilon-caprolactone) fibrous mats. *J Biomed Mater Res B Appl Biomater*. 2014;102(3):533–542. doi:10.1002/jbm.b.33032
12. Jones V, Grey JE, Harding KG. Wound dressings. *BMJ*. 2006;332(7544):777–780. doi:10.1136/bmj.332.7544.777
13. Schneider SW. Modern wound dressings. *J Dtsch Dermatol Ges*. 2012;10(6):383–385. doi:10.1111/j.1610-0387.2012.07955.x
14. Adkins CL. Wound care dressings and choices for care of wounds in the home. *Home Healthc Nurse*. 2013;31(5):259–67; quiz 268–9. doi:10.1097/NHH.0b013e31828eb658
15. Brassolatti P, Kido HW, Bossini PS, et al. Bacterial cellulose membrane used as biological dressings on third-degree burns in rats. *Biomed Mater Eng*. 2018;29(1):29–42. doi:10.3233/BME-171710
16. Lin WC, Lien CC, Yeh HJ, Yu CM, Hsu SH. Bacterial cellulose and bacterial cellulose-chitosan membranes for wound dressing applications. *Carbohydr Polym*. 2013;94(1):603–611. doi:10.1016/j.carbpol.2013.01.076
17. Kwak MH, Kim JE, Go J, et al. Bacterial cellulose membrane produced by *Acetobacter* sp. A10 for burn wound dressing applications. *Carbohydr Polym*. 2015;122:387–398. doi:10.1016/j.carbpol.2014.10.049
18. Kim J, Kim SW, Park S, et al. Bacterial cellulose nanofibrillar patch as a wound healing platform of tympanic membrane perforation. *Advan Healthc Mater*. 2013;2(11):1525–1531. doi:10.1002/adhm.201200368
19. Shao W, Wu J, Liu H, Ye S, Jiang L, Liu X. Novel bioactive surface functionalization of bacterial cellulose membrane. *Carbohydr Polym*. 2017;178:270–276. doi:10.1016/j.carbpol.2017.09.045
20. Slezak A, Jasik-Slezak J, Kucharzewski M. Biophysical properties of membrane dressing made of bacterial cellulose. *Polim Med*. 2005;35(2):15–21.
21. Shao W, Liu H, Liu X, et al. Development of silver sulfadiazine loaded bacterial cellulose/sodium alginate composite films with enhanced antibacterial property. *Carbohydr Polym*. 2015;132:351–358. doi:10.1016/j.carbpol.2015.06.057
22. Pal S, Nisi R, Stoppa M, Licciulli A. Silver-functionalized bacterial cellulose as antibacterial membrane for wound-healing applications. *ACS Omega*. 2017;2(7):3632–3639. doi:10.1021/acsomega.7b00442
23. Chi Z, Lin H, Li W, Zhang X, Zhang Q. In vitro assessment of the toxicity of small silver nanoparticles and silver ions to the red blood cells. *Environ Sci Pollut Res Int*. 2018;25(32):32373–32380. doi:10.1007/s11356-018-3217-2
24. Takamiya AS, Monteiro DR, Bernabe DG, et al. In vivo toxicity evaluation of colloidal silver nanoparticles used in endodontic treatments. *J Endod*. 2016;42(6):953–960. doi:10.1016/j.joen.2016.03.014
25. Elashmawi IS, Hakeem NA, Marei LK, Hanna FF. Structure and performance of ZnO/PVC nanocomposites. *Physica B*. 2010;405(19):4163–4169. doi:10.1016/j.physb.2010.07.006
26. Li LH, Deng JC, Deng HR, Liu ZL, Li XL. Preparation, characterization and antimicrobial activities of chitosan/Ag/ZnO blend films. *Chem Eng J*. 2010;160(1):378–382.
27. Espitia PJP, Soares NDF, Coimbra JSD, de Andrade NJ, Cruz RS, Medeiros EAA. Zinc oxide nanoparticles: synthesis, antimicrobial activity and food packaging applications. *Food Bioprocess Tech*. 2012;5(5):1447–1464.
28. Stankic S, Suman S, Haque F, Vidic J. Pure and multi metal oxide nanoparticles: synthesis, antibacterial and cytotoxic properties. *J Nanobiotechnology*. 2016;14(1):73. doi:10.1186/s12951-016-0225-6
29. Lansdown AB, Mirastschijski U, Stubbs N, Scanlon E, Agren MS. Zinc in wound healing: theoretical, experimental, and clinical aspects. *Wound Repair Regen*. 2007;15(1):2–16. doi:10.1111/wrr.2007.15.issue-1
30. Hu WL, Chen SY, Zhou BH, Wang HP. Facile synthesis of ZnO nanoparticles based on bacterial cellulose. *Mater Sci Eng B-Adv*. 2010;170(1–3):88–92. doi:10.1016/j.mseb.2010.02.034
31. Janpetch N, Saito N, Rujiravanit R. Fabrication of bacterial cellulose-ZnO composite via solution plasma process for antibacterial applications. *Carbohydr Polym*. 2016;148:335–344. doi:10.1016/j.carbpol.2016.04.066
32. Shah N, Ul-Islam M, Khattak WA, Park JK. Overview of bacterial cellulose composites: a multipurpose advanced material. *Carbohydr Polym*. 2013;98(2):1585–1598. doi:10.1016/j.carbpol.2013.08.018
33. Chang WS, Chen HH. Physical properties of bacterial cellulose composites for wound dressings. *Food Hydrocolloid*. 2016;53:75–83. doi:10.1016/j.foodhyd.2014.12.009
34. Xu R, Xia H, He W, et al. Controlled water vapor transmission rate promotes wound-healing via wound re-epithelialization and contraction enhancement. *Sci Rep*. 2016;6:24596. doi:10.1038/srep24596
35. Liu M, Liu T, Chen X, et al. Nano-silver-incorporated biomimetic polydopamine coating on a thermoplastic polyurethane porous nanocomposite as an efficient antibacterial wound dressing. *J Nanobiotechnology*. 2018;16(1):89. doi:10.1186/s12951-018-0416-4
36. Boateng JS, Matthews KH, Stevens HN, Eccleston GM. Wound healing dressings and drug delivery systems: a review. *J Pharm Sci*. 2008;97(8):2892–2923. doi:10.1002/jps.21210
37. GhavamiNejad A, Rajan Unnithan A, Ramachandra Kurup Sasikala A, et al. Mussel-inspired electrospun nanofibers functionalized with size-controlled silver nanoparticles for wound dressing application. *ACS Appl Mater Interfaces*. 2015;7(22):12176–12183. doi:10.1021/acsami.5b02542
38. Chiu CT, Lee JS, Chu CS, Chang YP, Wang YJ. Development of two alginate-based wound dressings. *J Mater Sci Mater Med*. 2008;19(6):2503–2513. doi:10.1007/s10856-008-3389-2
39. Gurgel LV, Junior OK, Gil RP, Gil LF. Adsorption of Cu(II), Cd(II), and Pb(II) from aqueous single metal solutions by cellulose and mercerized cellulose chemically modified with succinic anhydride. *Bioresour Technol*. 2008;99(8):3077–3083. doi:10.1016/j.biortech.2007.05.072
40. Moritz S, Wiegand C, Wesarg F, et al. Active wound dressings based on bacterial nanocellulose as drug delivery system for octenidine. *Int J Pharm*. 2014;471(1–2):45–55. doi:10.1016/j.ijpharm.2014.04.062
41. Fu F, Li L, Liu L, et al. Construction of cellulose based ZnO nanocomposite films with antibacterial properties through one-step coagulation. *ACS Appl Mater Interfaces*. 2015;7(4):2597–2606. doi:10.1021/am507639b
42. Sharifalhoseini Z, Entezari MH, Jalal R. Direct and indirect sonication affect differently the microstructure and the morphology of ZnO nanoparticles: optical behavior and its antibacterial activity. *Ultrason Sonochem*. 2015;27:466–473. doi:10.1016/j.ultsonch.2015.06.016
43. Russell AD. Similarities and differences in the responses of microorganisms to biocides. *J Antimicrob Chemother*. 2003;52(5):750–763. doi:10.1093/jac/dkg422

International Journal of Nanomedicine

Dovepress

Publish your work in this journal

The International Journal of Nanomedicine is an international, peer-reviewed journal focusing on the application of nanotechnology in diagnostics, therapeutics, and drug delivery systems throughout the biomedical field. This journal is indexed on PubMed Central, MedLine, CAS, SciSearch[®], Current Contents[®]/Clinical Medicine,

Journal Citation Reports/Science Edition, EMBase, Scopus and the Elsevier Bibliographic databases. The manuscript management system is completely online and includes a very quick and fair peer-review system, which is all easy to use. Visit <http://www.dovepress.com/testimonials.php> to read real quotes from published authors.

Submit your manuscript here: <https://www.dovepress.com/international-journal-of-nanomedicine-journal>